AIP | The Journal of Chemical Physics

Dynamics of anions and cations in cesium hydrogensulfide (CsHS, CsDS): Neutron and x-ray diffraction, calorimetry and proton NMR investigations

F. Haarmann, H. Jacobs, W. Kockelmann, J. Senker, P. Müller, C. A. Kennedy, R. A. Marriott, L. Qiu, and M. A. White

Citation: The Journal of Chemical Physics **117**, 4961 (2002); doi: 10.1063/1.1479141
View online: http://dx.doi.org/10.1063/1.1479141
View Table of Contents: http://scitation.aip.org/content/aip/journal/jcp/117/10?ver=pdfcov
Published by the AIP Publishing

Dynamics of anions and cations in cesium hydrogensulfide (CsHS, CsDS): Neutron and x-ray diffraction, calorimetry and proton NMR investigations

F. Haarmann[a] and H. Jacobs[b]
Fachbereich Chemie der Universität, AC I, D-44221 Dortmund, Germany

W. Kockelmann
Mineralogisch-Petrologisches Institut der Universität, D-53115 Bonn, Germany c/o ISIS, Rutherford Appleton Laboratory, Chilton OX11 0QX, United Kingdom

J. Senker
Department Chemie der LMU, Lehrstuhl für Anorganische Festkörperchemie, D-81377 München, Germany

P. Müller
Institut für Anorganische Chemie der RWTH, D-52056 Aachen, Germany

C. A. Kennedy, R. A. Marriott, L. Qiu, and M. A. White
Department of Chemistry, Dalhouse University, Halifax, Nova Scotia B3H 4J3, Canada

(Received 21 February 2002; accepted 26 March 2002)

Protonated and deuterated samples of the hydrogensulfide of cesium were studied by high-resolution neutron powder diffraction, calorimetry and proton NMR investigations in a wide temperature range. Primarily due to reorientational disorder of the anions, three modifications of the title compounds are known: an ordered low-temperature modification—LTM (tetragonal, I4/m, $Z=8$), a dynamically disordered middle-temperature modification—MTM (tetragonal, P4/mbm, $Z=2$), and a high-temperature modification—HTM (cubic, $Pm\bar{3}m$, $Z=1$). The LTM$\rightleftarrows$MTM phase transition is continuous. Its order parameter, related to an order/disorder and to a displacive part of the phase transition, coupled bilinearly, follows a critical law. The critical temperature $T_C=123.2\pm0.5$ K determined by neutron diffraction of CsDS is in good agreement with $T_C=121\pm2$ K obtained by calorimetric investigations. For the protonated title compound a shift to $T_C=129\pm2$ K was observed by calorimetric measurements. The entropy change of this transition is (0.24 ± 0.04) R and (0.27 ± 0.04) R for CsHS and CsDS, respectively. The MTM$\rightleftarrows$HTM phase transition is clearly of first order. The transition temperatures of CsHS and CsDS are $T=207.9\pm0.3$ K and $T=213.6\pm0.3$ K with entropy changes of (0.86 ± 0.01) R and (0.81 ± 0.01) R, respectively. Second moments (M_2) of the proton NMR absorption signal of MTM and HTM are in reasonable agreement with M_2 calculated for the known crystal structures. A minimum in spin-lattice relaxation times (T_1) in the MTM could not be assigned by dipolar coupling to a two-site 180° reorientation of the anions, a model of motion presumed by the knowledge of the crystal structure. The activation enthalpies determined by fits of T_1 presuming a thermal activated process are in the order of molecular reorientations ($E_a=13.5\pm0.5$ kJ mol^{-1} for the MTM and $E_a=9.3\pm0.3$ kJ mol^{-1} for the HTM). In the HTM at $T>330$ K translational motion of the cations determines T_1 ($E_a=13.8\pm0.4$ kJ mol^{-1}). © *2002 American Institute of Physics.* [DOI: 10.1063/1.1479141]

I. INTRODUCTION

The polymorphism of compounds is often linked to reorientational disorder of molecules or polyatomic ions. These may be asymmetric charged ions (OH^-,HS^-,CN^-), molecules (NH_3,H_2O) or molecules with a symmetric charge distribution (N_2,C_2^{2-}). Many properties such as moment of inertia, point symmetry, charge distribution, or the symmetry and the strength of coordination potential influence the dynamics of the molecules or ions. In the case of ionic compounds, the coordination potential often determines the motion of the ions.

The alkali metal hydrogensulfides (M^+HS^-/DS^-) are an ideal model system to study the influence of the cationic potential on the motion of the anions. Three modifications are known at ambient pressure for each of MHS with M = Na, K, Rb, Cs.[1,2] (The lithium compound[3] is an exception in the alkali metal hydrogensulfides and we did not include it into our investigations.) The anions are antiferroelectrically ordered in the low-temperature modifications (LTM) and two-site 180° reorientations of the anions are observed in the middle-temperature modifications (MTM). The cubic sym-

[a]Present address: Max-Planck Institut für Chemische Physik fester Stoffe, Nöthnitzer Str. 40, 01187 Dresden, Germany.
[b]Lehrstuhl für Anorganische Chemie I der Universität, 44221 Dortmund, Germany; electronic mail: Jacobs@pop.uni-dortmund.de

metry of the high-temperature modifications (HTM) is achieved by nearly free reorientation of the anions, highly influenced by the coordination potential. This is determined in first approximation by the cations. The three modifications of MHS with $M=$Na, K, Rb are isostructural for the different cations and related to the NaCl-type structure.[1] In contrast, the structures of CsHS are related to the CsCl-type structure.[2] No significant differences between protonated and deuterated hydrogensulfides of the alkali metals, besides a shift of the vibrational modes and the temperatures of the phase transitions, have been detected.

The alkali metal hydrogensulfides have been investigated in the past by x-ray and neutron diffraction to study their crystal structures.[1–5] The dynamics of the anions were analyzed by the use of IR/Raman spectroscopy,[6–9] inelastic and quasielastic neutron scattering,[10–12] and NMR,[13–16] but no systematic study of MHS with $M=$Na, K, Rb, Cs to characterize the influence of symmetry and strength of the coordination potential on the dynamics of the anions has been presented. This paper is a part of a series[17–20] focusing on the structure and the dynamics in these compounds. We used powder[17] and single crystal[19] neutron diffraction, quasielastic neutron scattering,[18] and ^{1}H-NMR[20] to study the hydrogensulfides of sodium, potassium, and rubidium. In this paper we present results regarding the hydrogensulfide of cesium, including neutron and x-ray diffraction, calorimetric investigations, second moments (M_2) of the NMR proton absorption signal and the NMR spin-lattice relaxation times (T_1) of the protons.

In addition to our main interest to characterize the reorientational dynamics of the anions in the hydrogensulfides of the alkali metals, we investigated the mechanism of the LTM$\rightleftarrows$MTM phase transition, because IR/Raman spectroscopic investigations[8] indicated a continuous transition, but no quantitative microscopic model could be drawn from these data. Furthermore, we focus on understanding the change of reorientational motion of the anions with temperature in the HTM, which was indicated by an IR/Raman spectroscopic study.[8]

In addition, CsHS and CsDS are the only hydrogensulfides of the alkali metals stabilized by hydrogen bonds.[8] Therefore the influence of hydrogen bonding on dynamics and structure was also of interest.

II. EXPERIMENTAL DETAILS

A. Preparation of samples

Cesium was purified by high vacuum distillation. Powder samples of colorless CsHS and CsDS were prepared by the reaction of Cs with H_2S and D_2S, respectively, at $T=323$ K in an autoclave manufactured from steel resistant against hydrogen sulfide as a corrosive gas (Alloy 556, Haynes International Inc., Kokomo, Indiana).[1] Hydrogen sulfide was produced by the reaction of Al_2S_3 (Sigma-Aldrich, Steinheim, Germany, 98%) with doubly distilled H_2O or D_2O (Center d'Etudes de Saclay, Gif-Sur-Yvette, France, 99.5%).[21]

The samples were handled under inert gas conditions[22] because they decompose on reaction with moisture. They were characterized by x-ray diffraction, IR, Raman, and DSC measurements to check for the presence of impurities. The amount of hydrogen in the deuterated sample was determined by NMR measurements to be H/D$<1\%$.

B. Diffraction

Neutron powder diffraction experiments were done at the time-of-flight (TOF) diffractometer ROTAX[23,24] at the pulsed spallation source ISIS, UK. With respect to the small scattering length of sulphur and the magnitude of the expected thermal motion of the ions, we increased the size of the sample to get satisfactory counting statistics within an acceptable time. About 15 g of CsDS was placed into a cylindrical vanadium container ($\phi=12$ mm), which was sealed with a gold gasket. To obtain the measurement temperature, $4\text{ K}\leqslant T\leqslant 400$ K, we used a ''cryofurnace'' device ($\phi=70$ mm) equipped with vanadium windows. The temperature was determined by a thermocouple mounted on the sample holder close to the sample. Vanadium has a very small coherent neutron scattering length. Therefore it produces negligible Bragg reflections, but the background radiation is increased by incoherent scattering. Two diffraction patterns, one in forward and one in backward scattering geometry, were detected simultaneously. The diffraction patterns were concurrently analyzed with the Rietveld refinement package GSAS.[25] We payed no attention to the small amount of hydrogen in our refinements by reducing the scattering length used for the deuterium sites to the weighted average of both isotopes. An empirical correction for absorption, which is primarily due to the absorption of cesium and vanadium, was used. To reduce the influence of correlation between thermal displacement parameters and absorption, the absorption coefficients were determined by simultaneous refinement of patterns obtained in the various modifications. The resultant coefficients were used for the analysis of all datasets.

The structure factors were extracted from the datasets with the GSAS package of programs. Standard Fourier synthesis and Fourier synthesis using Cesàro sums to reduce series cutoff effects were executed with the program Anaref.[26,27] The extracted structure factors obtained for the HTM were used in series expansions into symmetry adapted functions (SAF) to describe the nuclear probability density functions (pdf) of the anions.[28–31] Reflections with different sets of Miller indices fulfilling the relation $h_1^2+k_1^2+l_1^2=h_2^2+k_2^2+l_2^2$ were excluded.

X-ray powder diffraction of CsDS was carried out in the temperature range $190\text{ K}\leqslant T\leqslant 220$ K in steps of $\Delta T=2$ K. A Guinier diffractometer G645 (Huber, Rimsting, Germany) was used in transmission geometry with Cu$K\alpha_1$ radiation. The sample was covered by Kapton foil 200HN (thickness: 50 μm, August Krempel Soehne GmbH & Co., Enzweihingen, Germany). CsDS was diluted with Si as the internal standard for the lattice parameters and to prevent absorption. The temperatures were obtained using a closed cycle cryostat and determined by a calibrated Si diode situated close to the sample holder.

TABLE I. Crystallographic parameters obtained by Rietveld refinement of neutron diffraction patterns of CsDS (LTM: I4/m, $Z=8$; MTM: P4/mbm, $Z=2$; HTM: $Pm\bar{3}m$, $Z=1$). Refinements are based on split-atom models.

Modification T/K	LTM 4	LTM 100	MTM 170	HTM 220	HTM 280	HTM 340	HTM 400
a/Å	8.2020(1)	8.2268(2)	5.8465(1)	4.2880(1)	4.3052(1)	4.3271(1)	4.3449(1)
c/Å	9.0245(3)	9.0393(3)	4.5259(2)				
x(Cs)	0[a]	0[a]	0	$\frac{1}{2}$	$\frac{1}{2}$	$\frac{1}{2}$	$\frac{1}{2}$
y(Cs)	0[a]	0[a]	0	$\frac{1}{2}$	$\frac{1}{2}$	$\frac{1}{2}$	$\frac{1}{2}$
z(Cs)	0.2679(3)[a]	0.2647(4)[a]	0	$\frac{1}{2}$	$\frac{1}{2}$	$\frac{1}{2}$	$\frac{1}{2}$
$\langle u^2_{iso}(Cs)\rangle$/Å^2	0.0053(3)	0.0131(4)	0.0212(5)	0.0445(9)	0.056(1)	0.065(1)	0.073(1)
x(S)	0.2545(6)	0.2540(9)	0	0	0	0	0
y(S)	0.2425(6)	0.2424(8)	$\frac{1}{2}$	0	0	0	0
z(S)	0	0	$\frac{1}{2}$	0	0	0	0
$\langle u^2_{iso}(S)\rangle$/Å^2	0.0110(6)	0.0176(7)	0.0262(7)	0.0493(9)	0.0578(1)	0.070(1)	0.083(2)
x(D1)	0.0896(2)	0.0912(4)	0.1584(1)	0.2952(7)	0.2847(7)	0.2763(8)	0.2695(9)
y(D1)	0.2443(3)	0.2486(8)	$\frac{1}{2}+x$	0	0	0	0
z(D1)	0	0	$\frac{1}{2}$	0	0	0	0
occ(D1)[b]	0.974(2)	0.873(3)	1	1	1	1	1
$\langle u^2_{iso}(D1)\rangle$/Å^2	0.0295[c]	0.0368[c]	0.0453[c]	0.0821[c]	0.1004[c]	0.1210[c]	0.1349[c]
$\langle u^2_{xx}(D1)\rangle$/Å^2	0.019(1)	0.025(4)	0.035(1)	0.053(2)	0.072(2)	0.093(3)	0.110(4)
$\langle u^2_{yy}(D1)\rangle$/Å^2	0.031(2)	0.035(4)	0.043(2)	0.097(2)	0.115(2)	0.135(2)	0.147(3)
$\langle u^2_{zz}(D1)\rangle$/Å^2	0.039(1)	0.051(2)	0.058(2)	$\langle u^2_{yy}(D1)\rangle$	$\langle u^2_{yy}(D1)\rangle$	$\langle u^2_{yy}(D1)\rangle$	$\langle u^2_{yy}(D1)\rangle$
d(D1-S)/Å	1.353(5)	1.340(7)	1.309(2)	1.266(3)	1.224(3)	1.194(4)	1.171(4)
x(D2)	0.418[d]	0.418(3)					
y(D2)	0.224[d]	0.224(4)					
z(D2)	0	0					
$\langle u^2_{iso}(D2)\rangle$/Å^2	$\langle u^2_{iso}(S)\rangle$	$\langle u^2_{iso}(S)\rangle$					
d(D2-S)/Å	1.351(5)	1.359(2)					
α(D1-S-D2)/°	174.3(5)	176(1)					
$R_{F^2_0}$/%[e]	4.8/5.7	6.2/6.0	8.7/7.4	9.7/10.0	15.8/13.5	10.2/14.2	10.1/17.7
Q_f/Å^{-1}[f]	1.0–9.1	1.0–9.1	1.4–9.1	1.5–6.6	1.5–6.6	1.5–6.7	1.5–6.3
Q_b/Å^{-1}[f]	2.4–12.6	2.4–11.3	2.4–10.3	2.5–7.6	2.5–7.4	2.5–7.4	2.5–7.4

[a]Values for Cs2; the position of Cs1 is (0 $\frac{1}{2}$ $\frac{1}{4}$).
[b]Occupation of the deuterium positions is fixed to occ(D1)+occ(D2)=1.
[c]Calculated from results of anisotropic refinement.
[d]Not refined.
[e]Detector in forward/backward scattering geometry.
[f]$Q_{min} \leqslant Q_X \leqslant Q_{max}$, with X as the number of the detector.

C. Calorimetric investigations

The heat capacities of CsHS and CsDS (sample masses 4.570 and 4.552 g, respectively) were determined from about $T=30$ K to $T=300$ K by adiabatic heat pulse calorimetry, as described in detail elsewhere.[32] Briefly, the sample, in a sealed calorimeter, was increased in temperature by quantified Joule heating, while adiabatic conditions were maintained. The temperature was monitored with a platinum resistance thermometer, and the temperatures before and after application of the heat pulse were determined. The heat capacities of the calorimeter and its addenda were determined in separate experiments, and subtracted from the total heat capacity to give the heat capacity of the sample. The uncertainty of the heat capacity determined in this way has been found to be within $\pm 0.5\%$ (Ref. 32).

D. NMR

Powder samples of CsHS were sealed into standard NMR tubes (ø5 mm). The temperatures $150\ \text{K} \leqslant T \leqslant 540\ \text{K}$ were obtained by the use of a N_2 gas flow system on an MSL 400 NMR spectrometer (Fa. Bruker Physik, Karlsruhe, Germany). They were measured with a platinum resistance thermometer fixed in a distance of 1 cm from the sample coil. The experiments were done at a proton resonance frequency $\nu_0=400$ MHz.

The spectra for an analysis of M_2 were detected by a solid-echo pulse sequence to reduce the influence of dead time of the sample coil. To ensure that the decay of the echo represents the FID of the signal we optimized the separation of pulses (τ) by a variation of $\tau=10$, 20, 30, 40, and 50 μs. For the final measurement, $\tau=20$ μs was used. To reduce the influence of noise in the signal, we fitted the spectra using a sum of Gaussian and Lorentzian lines to determine M_2. A saturation recovery technique with a single 90° pulse for detection was applied to measure T_1. A random variation of the waiting periods between saturation and detection pulses prevents systematic errors caused by slight shifts of temperature.

III. RESULTS AND DISCUSSION

A. Diffraction

Neutron powder diffraction experiments on CsDS were carried out in order to get information about the pdf of the atoms, especially deuterium. In addition, x-ray powder dif-

fraction was used to study the lattice parameters of CsDS close to the MTM⇄HTM phase transition as a function of temperature.

1. HTM

The crystal structure of the cubic HTM of cesium hydrogensulfide is related to the CsCl-type structure (space group: $Pm\bar{3}m$, $Z=1$). Sulphur and cesium atoms occupy the positions of the ions in CsCl. The anions are reorientationally disordered. Averaged over time, the anions are preferentially aligned parallel to the cubic axes. IR/Raman investigations[8,33] indicate a change in the anion motion with temperature within the HTM. This was concluded from the temperature-dependent development of the line shape of the stretching mode ν(HS). Therefore a partial occupation of Wyckoff positions 6e, 8g, and 12i by hydrogen has been discussed.[1,8] To study this in some detail we did neutron powder diffraction on fully deuterated samples at several temperatures in the HTM.

We analyzed the diffraction patterns using standard split-atom models, Fourier synthesis, and SAF. The following split-atom models were used to take the pdf of deuterium into consideration, keeping the total number of D atoms fixed to the composition of the compound.

(I) Exclusive occupation of Wyckoff positions 6e, 8g, or 12i, assuming anisotropic displacement of deuterium.

(II) Partial occupation of the sites 6e, 8g, and 12i within one model assuming isotropic displacement of D. The parameters of the deuterium positions were constrained to ensure the same interatomic distance between D and S for the different sites. Displacement parameters of the three sites were constrained to have the same value. The deuterium occupation numbers of the different sites were refined.

The data analysis shows that for $T \lesssim 300$ K model (I) with an exclusive occupation of Wyckoff position 6e is clearly favored. For temperatures above 300 K, results of model (I) cannot be distinguished on the basis of goodness of fit criteria from results of model (II), considering partial occupation of sites 6e, 8g, and 12i. The refinements yield for model (II) occupancies of the sites $12i(5\%) < 8g(15\%) < 6e(80\%)$ that are not temperature dependent. Model (II) involves a higher population of electrostatic unfavored positions, where the anions point with the positive end (deuterium) toward the cations. Therefore, the occupation of only one site, 6e, is more likely for the whole HTM temperature range. Refinement results are given in Table I for four temperatures in the HTM. These results of refinement are confirmed by Fourier analysis using observed structure factors that were obtained from the neutron diffraction patterns on the basis of the different 6e-, 8g-, and 12i-site models. No significant maxima corresponding to sites 8g and 12i were observed. Only maxima for an alignment of the anions parallel to the cubic axis pointing toward the faces of the anion coordination polyhedra (Fig. 1) were found in agreement with a sole deuterium occupation of site 6e.

In addition, we developed the extracted structure factors into SAF. We described this procedure in detail in Ref. 17. The momentum transfer of our measurements allows refinement of the coefficients c_{41}, c_{61}, and c_{81} of the related SAF.

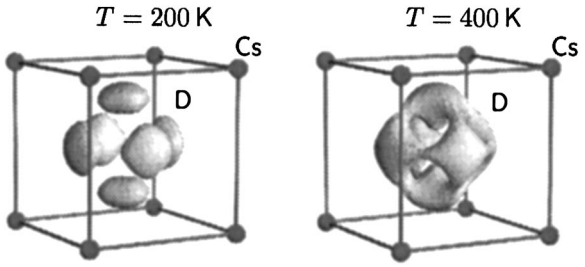

FIG. 1. CsDS at $T=220$ K and $T=400$ K: The probability density function (pdf) of deuterium from the refinement of neutron diffraction data using SAF. Sulphur is omitted and the probability density of the cations deliberately reduced for clarity.

But the results for c_{81} did not differ significantly from their estimated standard deviation. Therefore we neglected this parameter ($c_{81}=0$). Due to large correlations between thermal parameters of the anions and the bond length, we fixed the distance to values determined by the Rietveld refinement (Table I). The results of these SAF refinements are summarized in Table II. The coefficient c_{41} is almost constant whereas c_{61} increases with temperature. While the thermal displacement parameters of Cs obtained from Rietveld refinement and SAF analysis are in agreement within the estimated error; those of sulphur and of the whole anion are not. The overall thermal displacement parameter of the anion using SAF should correspond to the parameter of sulphur determined by Rietveld refinement. The overall displacement of the anion must be similar to that of the center of mass. The discrepancies in the thermal displacement parameters as well as the correlation between the displacement parameter and the bond length of the anion imply coupling of its translational and rotational motion of the anion in the HTM. In Fig. 1, a three-dimensional representation of the pdf of deuterium is given for two temperatures with respect to the coordination polyhedron.

The quality of the refinements is slightly better for the SAF than for the split-atom model. The SAF model seems to be more appropriate to describe the pdf of D in the HTM of CsDS. Compared to the split-atom models, the pdf of D determined by SAF is much more smeared out (Fig. 1). The SAF analysis allows an orientation of the anion along ⟨110⟩. The probability for this orientation rises with increasing temperature.

TABLE II. Crystallographic parameters obtained by least-squares refinement of structure factors of neutron diffraction patterns of CsDS (HTM). Refinement based on symmetry-adapted functions (SAF).

CsDS	220 K	280 K	340 K	400 K
$\langle u^2_{iso}(Cs)\rangle/Å^2$	0.049(3)	0.062(6)	0.066(5)	0.075(6)
$\langle u^2_{iso}(DS)\rangle/Å^2$	0.058(4)	0.081(9)	0.089(9)	0.11(1)
c_{41}[a]	1.9(1)	1.6(2)	1.5(2)	1.7(2)
c_{61}[a]	0.52(9)	0.6(2)	0.6(2)	1.0(4)
$R_{F_0^2}$/%	9.2	13.3	12.9	12.0

[a]Coefficients of cubic harmonics (Ref. 28).

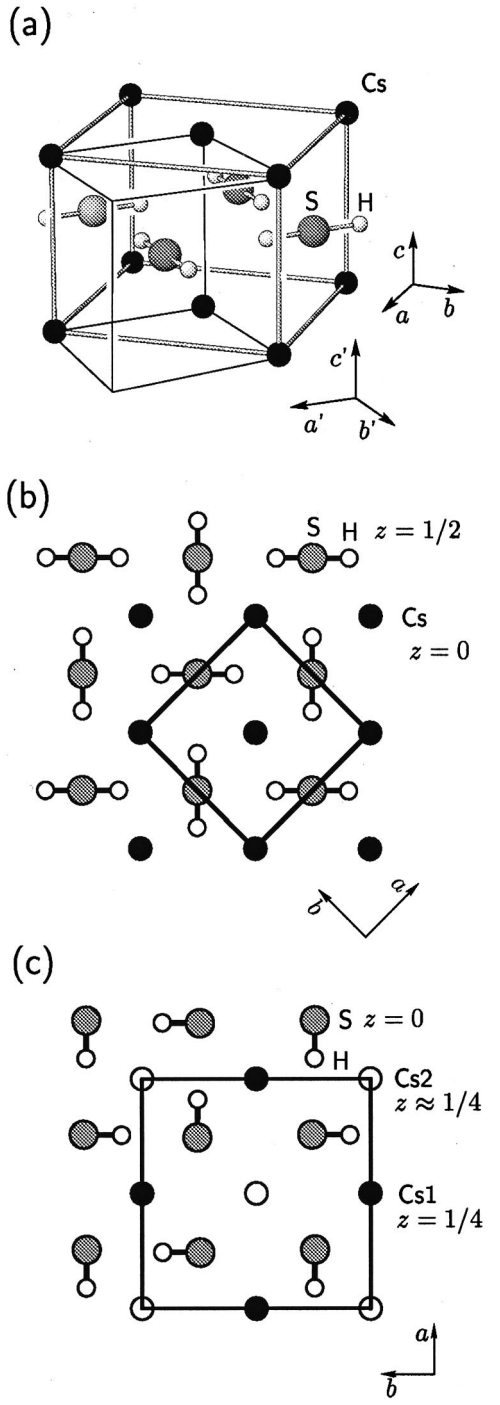

FIG. 2. (a) Unit cell of the MTM (a,b,c) of CsHS with respect to the cubic cell of the HTM (a',b',c') that is shifted by (0, $\frac{1}{2}$, $\frac{1}{2}$). (b) and (c) a,b plane of CsHS in the MTM and LTM, respectively. Unit cells are marked.

2. MTM

The crystal structure of the MTM of CsHS is tetragonal (space group: P4/mbm, $Z=2$) and related to the CsCl-type structure [Fig. 2(a)]. A two-dimensional net of hydrogen bonds is built in the a,b plane of the unit cell [Fig. 2(b)]. The anions are reorientationally disordered; both positions of hydrogen are equivalent and occupied with $\frac{1}{2}$ probability.

The patterns of the MTM obtained by the neutron diffraction of CsDS were refined using standard split-atom models. A considerable anisotropy of the pdf of deuterium must be taken into account in order to reach satisfactory results. As a representative for the whole MTM regime, the results of Rietveld refinements for $T=170$ K are summarized in Table I.

For $T<170$ K diffuse scattering arises at $d\approx 3.41$ Å, which is close to the d spacing of the (1 2 1) reflection of the LTM. This reflection is sensitive to the order of the anions and indicates short-range order at the lower-temperature end of the MTM.

3. LTM

As for the MTM, the LTM of CsHS is tetragonal (space group: I4/m, $Z=8$), but with a larger unit cell. To a first approximation, the anions are antiferroelectrically ordered at $T=4$ K forming cyclic $S_4H_4^{4-}$ groups with S–H···S–H hydrogen bonds [Fig. 2(c)]. Two inequivalent positions of Cs exist. While the position of Cs1 has no positional parameter to be refined, the position of Cs2 has a free z parameter. The inequality of the Cs sites arises from the arrangement of the anions: Both cations are coordinated by eight anions, which are grouped into two planar cyclic $S_4H_4^{4-}$ units orientated parallel to the a,b plane of the unit cell. Cs1 at $z=\frac{1}{4}$ is coordinated by two equivalent $S_4H_4^{4-}$ groups that are characterized by anions with hydrogen atoms pointing onto sulphur atoms inside the group. On the other hand, Cs2 is coordinated by two inequivalent $S_4H_4^{4-}$ units with anions that either all point with the hydrogen atoms onto sulphur atoms within the unit, or that all points with the hydrogen atoms onto sulphur atoms outside the group [Fig. 2(c)]. Therefore Cs2 shifts away from the $z=\frac{1}{4}$ position, driven by different electrostatic interactions of the closed and the open $S_4H_4^{4-}$ rings.

To avoid correlations of the thermal displacement parameters of both Cs sites, we constrained these parameters in our Rietveld refinements of neutron powder diffraction data. Patterns obtained at $T=4$ K and $T=100$ K differ significantly and a weakening of superlattice reflections of the LTM with increasing temperature can be seen [Fig. 3(a)]. The temperatures of the LTM$\rightleftarrows$MTM phase transition were estimated by Raman scattering[8] as $T_C=118$ K and $T_C=103$ K for CsHS and CsDS, respectively. From the calorimetric results (*vide infra*), we see that at $T=100$ K, the LTM$\rightleftarrows$MTM has already begun.

The differences in the diffraction patterns indicate a change of the crystal structure with temperature. A model of the crystal structure that accounts for the change near the phase transition temperature has been derived from Fourier analysis [Fig. 3(b)]. A second, partially occupied D2 position is introduced to approximate the crystal structure of the MTM. Results of Rietveld refinements are summarized in Table I. Even for $T=4$ K, a small occupation of position D2 is determined. This might be due to correlations of parameters in the Rietveld refinements or due to the presence of a residual static disorder. We did a series of short neutron diffraction measurements in order to record the temperature dependence of the D2 occupation and the Cs2 positional shift. To refine these patterns we constrained the thermal displacement parameters of D2 to that of sulphur and constrained the parameters of the position of D2 to values determined for

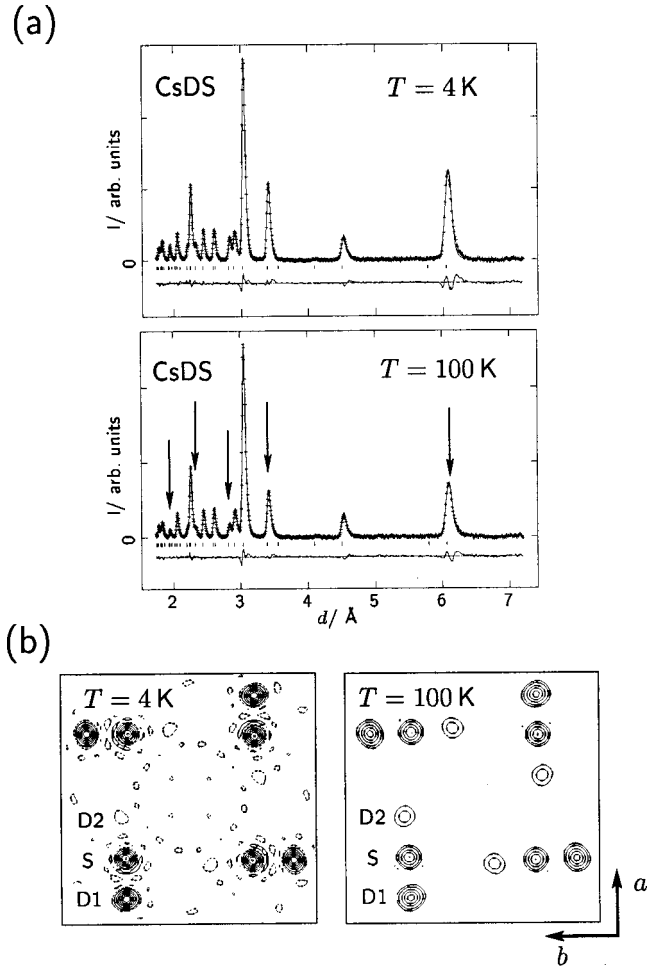

FIG. 3. (a) Neutron diffraction pattern of CsDS at $T=4$ K and $T=100$ K (LTM). The positions of weakened reflections are marked. The background was subtracted to focus on the change in intensity. (b) Fourier maps of the *a*,*b* plane with $z=0$ of CsDS obtained from the neutron diffraction pattern at $T=4$ K and $T=100$ K. Dotted lines indicate pdf$\leqslant 0$; full lines pdf>0.

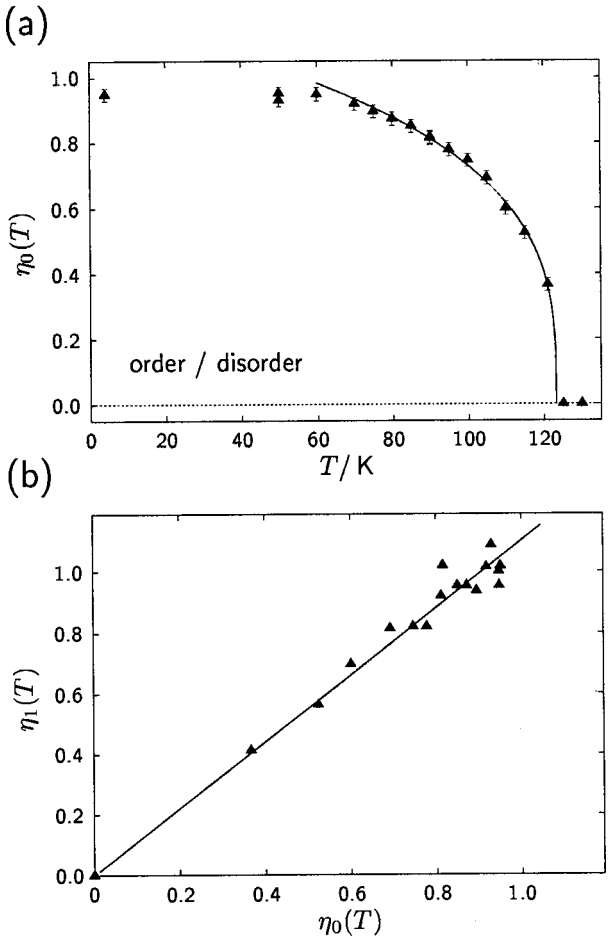

FIG. 4. (a) Primary order parameter [Eq. (1)] of CsDS as a function of temperature $\eta_0(T)=1-2\cdot\mathrm{occ}$, with occ as the fractional occupation of position D2. The full line indicates the critical law fitted to η_0. (b) Secondary vs primary order parameter (displacive η_1 and order/disorder η_0).

$T=100$ K. In addition, we fixed the sum of the fractional occupations of D1 and D2 [occ(D1)+occ(D2)=1]. The resultant parameters did not depend on whether the measurement temperature was approached by heating or cooling of the sample.

Two order parameters were introduced to characterize the LTM$\rightleftarrows$MTM phase transition. A primary order parameter $\eta_0(T)$ describing the order/disorder part of the phase transition and depending on the occupation of D2 was defined as

$$\eta_0(T)=1-2\cdot\mathrm{occ(D2)}. \tag{1}$$

In addition, an order parameter $\eta_1(T)$ is related to the shift of Cs2:

$$\eta_1(T)=\frac{\Delta z_{\mathrm{Cs2}}(T)}{\Delta z_{\mathrm{Cs2\ max}}(T)}, \tag{2}$$

with $\Delta z_{\mathrm{Cs2}}(T)=z_{\mathrm{Cs2}}(T)-\frac{1}{4}$. This order parameter is related to the displacive part of the phase transition.

The temperature dependence of $\eta_0(T)$ is presented in Fig. 4(a). The order parameter of the order/disorder part follows a critical law:[34]

$$\eta(T)=f\cdot\left(\frac{T_C-T}{T_C}\right)^n, \tag{3}$$

with $T_C=123.2\pm0.5$ K as the critical temperature, $f=1.20\pm0.02$ as a scaling factor, and $n=0.30\pm0.02$ as the critical exponent for CsDS [Fig. 4(a)]. The diffraction patterns are less sensitive to the shift of Cs2, but the results of a fit of $\eta_1(T)$ using a critical law agrees well within the estimated standard deviations to those of $\eta_0(T)$ ($T_C=122\pm2$ K, $f=1.18\pm0.09$, $n=0.26\pm0.06$). The bilinear coupling of the primary order parameter $\eta_0(T)$ and the so-called pseudoprimary order parameter[35] $\eta_1(T)$ are presented in Fig. 4(b). The coupling of the order parameters supports the hypothesis that the shift of Cs2 is due to electrostatical interactions. These are averaged out by the increasing disorder with rising temperature.

4. Temperature dependence of lattice and thermal displacement parameters

While the LTM$\rightleftarrows$MTM transition is continuous, the MTM$\rightleftarrows$HTM transition is of first order. The volume increases at the MTM$\rightleftarrows$HTM transition by about 1%, as also found for *M*DS with *M*=Na,K,Rb.[36] Hysteresis of the transition of about $\Delta T=6$ K was detected using powder x-ray

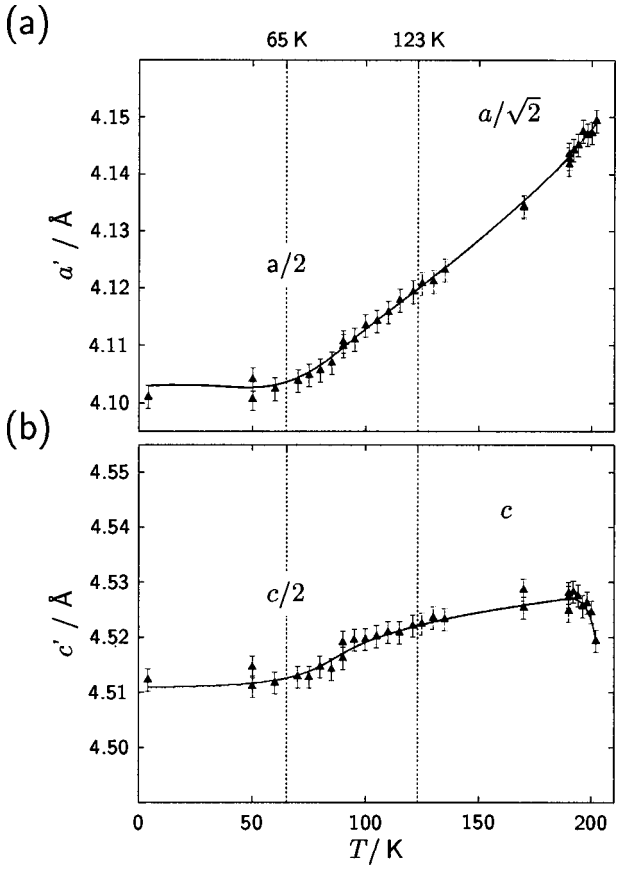

FIG. 5. Lattice parameters of CsDS as a function of temperature for the LTM and MTM. (a) a' and (b) c'. The phase transition at $T=123$ K and the beginning of observed disorder at $T=65$ K are marked by dotted lines. Full lines represent a guide to the eye.

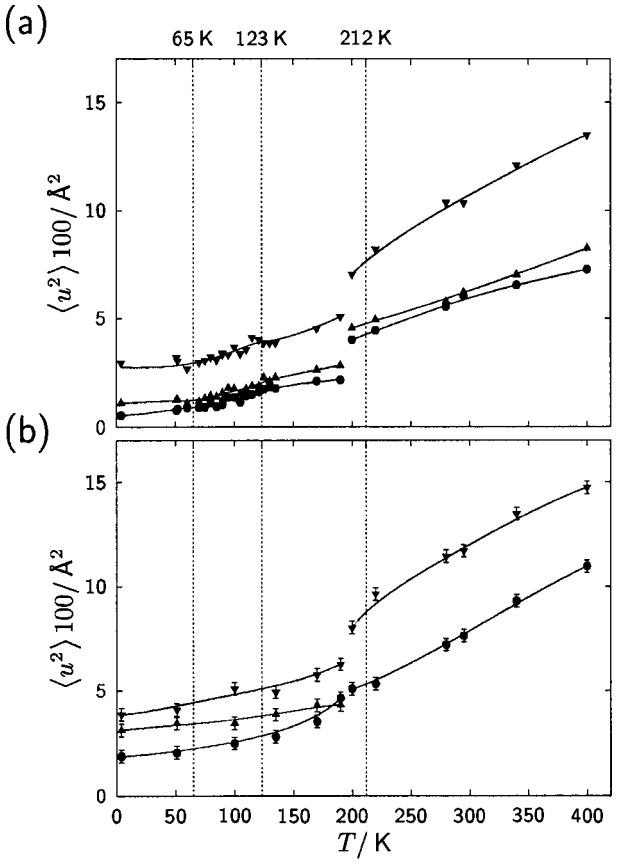

FIG. 6. Thermal displacement parameters of CsDS as a function of temperature. (a) Isotropic displacement, ▼: D calculated from refinement of anisotropic displacement, ▲: S, ●: Cs and (b) principal axis of anisotropic deuterium displacement parameters, ●: $\langle u_x^2\rangle$, ▲: $\langle u_y^2\rangle$, ▼: $\langle u_z^2\rangle$. The temperatures of the phase transitions and the beginning of observed disorder at $T=65$ K are marked by dotted lines. Full lines represent a guide to the eye. Points at $T=200$ K belong to the HTM.

diffraction. For heating CsDS in the temperature range $202\ \text{K} \leqslant T \leqslant 210\ \text{K}$, both modifications were observed simultaneously. The amount of the HTM increases with temperature, detected by the rising intensity of the reflections of the HTM. For cooling of the sample, a similar behavior was observed.

A distinct precursor effect of the lattice parameters can be seen in the c/a ratio that approximates cubic symmetry at temperatures close to the MTM→HTM phase transition.

With the onset of orientational disorder of the anions at the beginning of the LTM→MTM phase transition at $T \approx 65$ K, an increase of the lattice expansion was detected (Fig. 5). Whereas the a parameter above $T \approx 65$ K grows linear up to the phase transition MTM→HTM [Fig. 5(a)], the expansion along the c axis in the interval $65\ \text{K} \leqslant T \leqslant 110\ \text{K}$ has a significant higher slope [Fig. 5(b)], but about 10 K below the MTM→HTM transition it decreases with increasing temperature.

The isotropic thermal displacement parameters of the atoms of CsDS determined by Rietveld refinement of the neutron diffraction pattern are presented in Fig. 6(a). In the temperature range $65\ \text{K} \leqslant T \leqslant 123\ \text{K}$, just below the LTM→MTM phase transition, a sharp increase of thermal displacement parameters with temperature was observed. The thermal parameters of all the atoms show the same behavior around the MTM⇄HTM phase transition. In this respect CsDS behaves distinctly at the MTM⇄HTM phase transition, different from NaDS and KDS, both of which display a much larger rise of the cation displacement parameters than the thermal parameters of D and S (Ref. 17).

The anisotropy of the thermal displacement of deuterium is significant [Fig. 6(b)]. The motion of the anions can be separated into a reorientational jump process and reorientations of relative small amplitude and the translation of small amplitude. The reorientations of small amplitude are due to librational motions and in a first approximation they are represented by the thermal displacement parameters of deuterium. These can be distinguished in the LTM and MTM by $\langle u_z^2\rangle$ and $\langle u_y^2\rangle$ for motion parallel to the c axis and within the a,b plane of the unit cell, respectively. While the amplitude of the translational motion, approximately $\langle u_x^2\rangle$, increases nonlinearly with temperature, the amplitudes of librational motion increase linearly with temperature. At the MTM⇄HTM phase transition, there is a continuous crossover of the translational amplitude curve, but with a distinct change of gradient at the transition temperature [Fig. 6(b)]. However, the amplitudes of the librational motions, which are symmetry equivalent in the HTM, undergo an instantaneous jump at the MTM⇄HTM transition temperature.

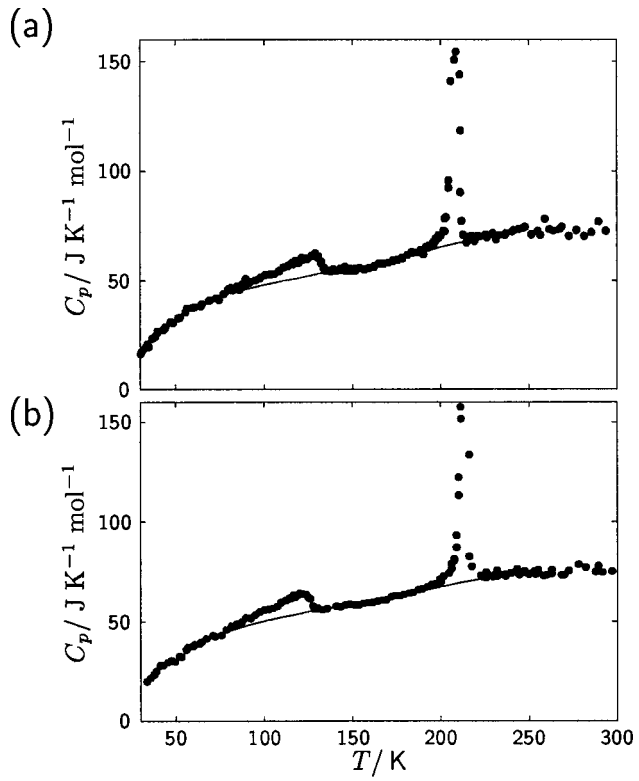

FIG. 7. The heat capacity of (a) CsHS and (b) CsDS as a function of temperature. The circles denote the experimental data and the full lines show the baseline heat capacity in the region of the phase transitions.

B. Calorimetric investigations

The heat capacities of CsHS and CsDS, shown in Figs. 7(a) and 7(b), respectively, both show the same main features, namely a lower-temperature phase transition with a significant gradual component, and a higher-temperature phase transition that is much sharper. (The experimental data have been deposited and are available through EPAPS.) The enthalpy and entropy changes at the lower-temperature transition were determined by direct integration, and over the sharper high-temperature transition these were determined by the ''long heat'' method.[37] The differences between the heat capacities of CsHS and CsDS are rather small. In general, and certainly above $T=70$ K, the heat capacity of CsDS is a little larger than that of CsHS (e.g., by about 5% at $T=160$ K), as one would expect based on the more massive deuterated salt having more closely spaced vibrational energy levels. The shift in transition temperature and enthalpy and entropy change on deuteration is also rather minor (Table III), with CsDS having the longer range for the MTM

TABLE III. Phase transition summary for CsHS and CsDS based on calorimetric studies. R is the gas constant.

	$T_{\rm trs}$/K	$\Delta_{\rm trs}H$/J mol^{-1}	$\Delta_{\rm trs}S/R$	Comments
CsHS	129±2	260±40	0.24±0.04	Higher order
	207.9±0.3	1492±8	0.86±0.01	First order
CsDS	121±2	270±40	0.27±0.04	Higher order
	213.6±0.3	1440±20	0.81±0.01	First order

owing to the lower LTM⇄MTM transition temperature and a higher MTM⇄HTM phase transition temperature. (It is only possible to do the calorimetric experiments in the heating mode, so they do not give information about hysteresis.) The similarities in transition temperature and entropy change indicate that most likely both CsHS and CsDS have very similar origins for the LTM⇄MTM and the MTM⇄HTM transition, in contrast with, for example, sodium hydroxide in which deuteration adds an additional phase transition.[38] The shapes of the calorimetric curves for CsHS and CsDS indicate that the higher-temperature transition is first order, and the lower-temperature transition is of higher order. These results are in agreement with the present diffraction data.

From the diffraction studies presented above, it is known that the LTM has the anions antiferroelectrically ordered, although reorientational disorder sets in well below the LTM →MTM phase transition. In addition, there is displacive shift of the Cs^+ ions in LTM. In the MTM, the anions are reorientationally disordered, with two equivalent H (or D) positions, both occupied with 50% probability. If the LTM →MTM phase transition was simply a matter of the onset of two-fold dynamical disorder of the HS^- (or DS^-) ions, the associated entropy change would be $\Delta_{\rm trs}S=R\ln 2=0.69$ R, considerably more than observed [$\Delta_{\rm trs}S=(0.24\pm0.04)$ R for CsHS and (0.27 ± 0.04) R for CsDS]. That the observed entropy change is less than $R\ln 2$ is consistent with the diffraction experiments, which show some residual anion disorder in LTM and some short-range ordering of the anions well above the LTM→MTM phase transition.

For each of CsHS and CsDS, the excess heat capacity at the lower-temperature transition, ΔC_p, determined by subtraction of the baseline heat capacity [Figs. 7(a) and 7(b)] from the experimental heat capacity, was fit to the function

$$\Delta C_p = f' \left| \frac{T_C - T}{T_C} \right|^n , \tag{4}$$

and the best fit (Fig. 8) was found with $n=0.3$ ($T_C=129$ K for CsHS and $T_C=121$ K for CsDS), in good agreement with the fit for the CsDS neutron powder diffraction experiments (*vide supra*). The observed transition is not as sharp as the calculated critical heat capacity fit, but this rounding is not unusual and could be associated with a distribution of domains in such a large sample.[39]

From the diffraction studies and NMR second-moment analyses, the high-temperature phase appears to have increased anionic disorder, well described by a six-site jump process. On the basis of an increase from two-site disorder in MTM to six-site disorder in HTM, and an increase in volume of about 1% at the MTM→HTM phase transition (Sec. III A 4), one would expect a transition entropy change of $\Delta_{\rm trs}S=R\ln(6/2)+R\ln(1.01)=1.1$ R, where the dynamical disorder contribution is about 100 times that of the volume increase. This estimate of $\Delta_{\rm trs}S$ is about 30% greater than observed [(0.86 ± 0.01) R for CsHS and (0.81 ± 0.01) R for CsDS], in line with the finding from the NMR spin-lattice relaxation studies (Sec. III C 2) that there is more disorder in the MTM than described by the two-site model.

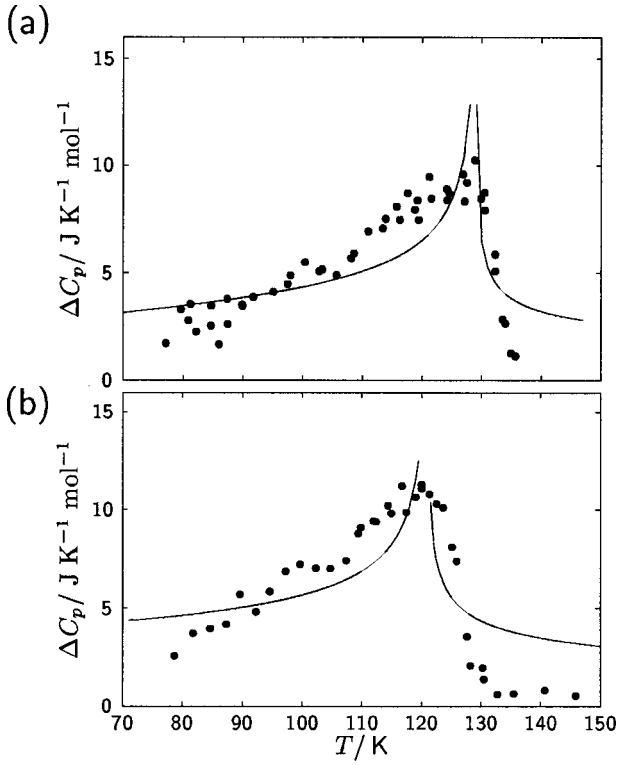

FIG. 8. Critical exponent fit to the excess heat capacity, ΔC_p at the lower-temperature phase transition in (a) CsHS and (b) CsDS.

C. NMR

The structural and especially dynamical properties of CsHS were investigated by proton NMR. We used the method of the second moments (M_2) and analyzed the spin-lattice relaxation times (T_1). Dipolar coupling of the spins was assumed to be the dominant interaction and therefore only Cs–H and H–H coupling were considered in our calculations. With the small natural abundance of ^{33}S, sulphur has no relevant contribution to the dipolar interaction of the system.

1. Second moments

Proton spectra of CsHS measured at several different temperatures are presented in Fig. 9(a). In contrast to the proton NMR signal of MHS with M=Na, K, Rb, where a small anisotropy of the chemical shielding tensor was observed,[20] the comparable signals of CsHS are symmetric. At the MTM⇄HTM phase transitions, a small drop of the signal width was observed. At the highest temperatures in the HTM, the signal becomes Lorentzian-like.

The formalism and calculations of M_2[20] are based on the crystal structures and parameters described in Sec. III A (see Table I for LTM: T=4 K, MTM: T=170 K, and HTM: T=220 K). The motion of the anions was related to a six- and a two-site jump process of the protons for the HTM and MTM, respectively. The calculations for the LTM are based on the idealized ordered modification considering only one site for the protons. The results of the calculations and the analysis of the absorption signal are summarized in Table IV. The calculations and the observed signal are in reasonable agreement.

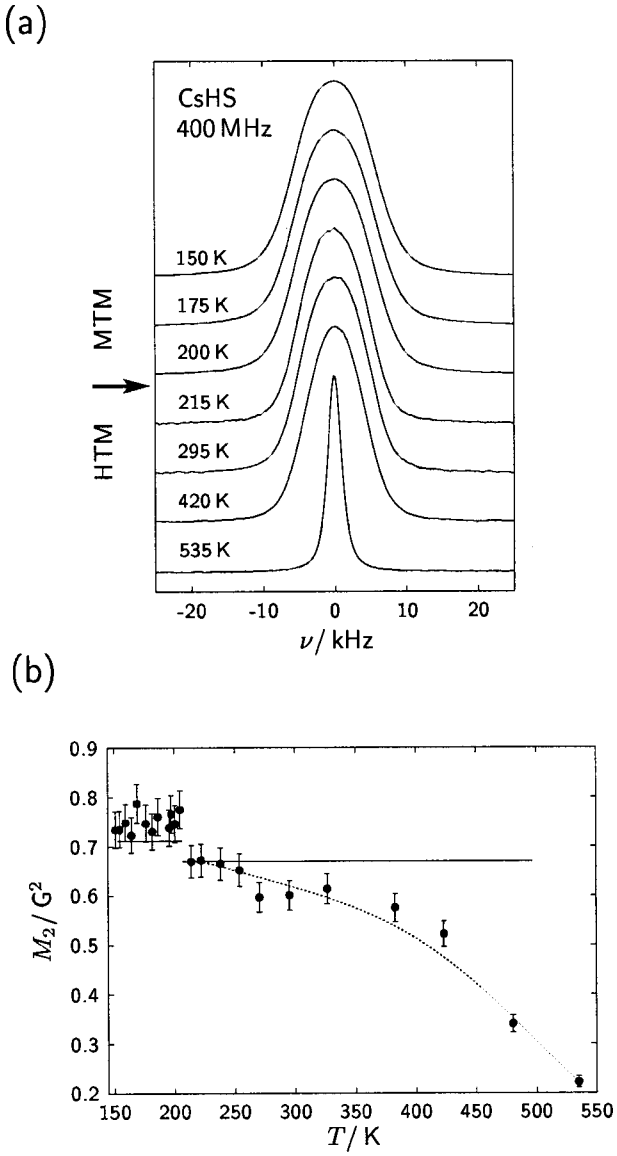

FIG. 9. (a) Proton NMR spectra of CsHS at various temperatures. The spectra are scaled to unity and shifted by a small offset. The temperature of the MTM⇄HTM phase transition is marked. (b) Second moments (M_2) of CsHS calculated from the absorption signal. The error bars indicate an uncertainty of ±5%. Full lines indicate M_2 calculated for the known structure of CsDS at T=220 K and T=170 K (Secs. III A 1 and III A 2). The dotted line represents a guide to the eye.

In the case of the MTM, the arithmetic average of the second moments determined from the spectra is about 6% higher than the calculated M_2 [Fig. 9(b)]. Assuming that CsHS and CsDS are similar in their physical properties, the influence of lattice expansion on M_2 within the MTM is about ±1%. A systematic decrease of M_2 with temperature in the MTM was not observed. For the HTM the width of the signal decreases significantly with rising temperature, much more than expected by lattice expansion. As a consequence, observed and calculated M_2 values should be compared for the lowest temperature point measured in the HTM. M_2 calculated from structure parameters of CsDS, obtained by neutron powder diffraction at T=220 K and T=400 K, reduces with increasing temperature by about 8%. In the same temperature range M_2 of the signal reduces by about 77%.

TABLE IV. Second moment (M_2) calculated from the proton absorption signal (O) and for the known crystal structures (C). The structure models were based on the results of neutron diffraction experiments (LTM, $T=4$ K; MTM, $T=170$ K; HTM $T=220$ K; see Sec. III A).

Modification	$M_{2(C)}/G^2$	$M_{2(O)}/G^2$
LTM	1.510	-[a]
MTM	0.711	0.75 ± 0.2[b]
HTM	0.675	0.67[c]

[a]Not within the investigated temperature range.
[b]Mean value of all measurements in MTM.
[c]Maximum of the observed values in HTM.

TABLE V. Observed (O) and calculated (C) minima of spin-lattice relaxation times (T_1). The structure models were based on results of neutron diffraction on CsDS (MTM, $T=170$ K; see Sec. III A 2). In addition, two-site 180° reorientations of the anions were considered. Different models were used to describe the correlated and uncorrelated motion of the anions.

Model	$T_{1\ \min(C)}$/s	$\tau_c/10^{-10}$ s
Uncorrelated	7.620	5.869
Ferroelectrical	8.262	5.803
Antiferroelectrical	7.629	5.629
$T_{1\ \min(O)}=5.6\pm0.6$ s		

Therefore a motional process other than reorientations of the anions must influence the linewidth of the signal.

2. Spin-lattice relaxation

The temperature dependence of T_1 is shown by an Arrhenius plot in Fig. 10. Exponential relaxation of the longitudinal magnetization was observed at all temperatures. The minimum of T_1 at $T=201$ K in the MTM is at slightly lower temperatures than for RbHS, which has the lowest temperature of the T_1 minima of the isotypic hydrogensulfides MHS with $M=$ Na, K, Rb[20] ($\nu_0=400$ MHz).

Calculations based on results of the neutron diffraction experiments on CsDS at $T=170$ K (Sec. III A 2) were carried out using different jump models to describe the reorientational dynamics of the anions. We chose $d=1.34$ Å (Ref. 40) as the bond length of the anion for our calculations in order to ensure comparable results for different models. The basics of these calculations are presented in Ref. 20 and we omit a repetition here.

Results of our calculations considering two-site 180° reorientations of the anions in MTM are summarized in Table V. The agreement of calculated and observed T_1 is unsatisfactory, whether or not correlated or uncorrelated motion of the anions was taken into account. Correlated motion means a collective reorientation of the ions, presuming a definite start orientation of the anions. The differences between T_1 observed and calculated for the various models is between 36% and 48%. The outcome of the calculations is not very sensitive to the lattice parameters and the bond length d(HS). A change of lattice parameters by ±1% leads to a change of $T_{1\ \min}$ of about ±8% and a reduction of the bond length of the anions from $d=1.34$ Å to $d=1.24$ Å increases $T_{1\ \min}$ by about 14%. Even including the uncertainties of structure determination, we are not able to explain the observed T_1 by two-site 180° reorientations of the anions in the MTM.

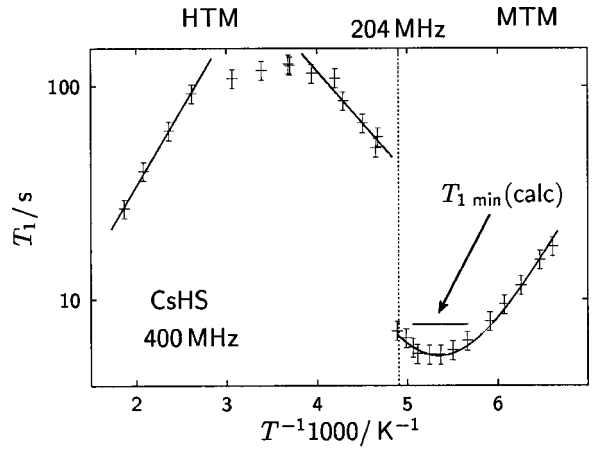

FIG. 10. Arrhenius plots of spin-lattice relaxation times (T_1) of CsHS. The error bars indicate an estimated uncertainty of ±10% in T_1. The temperature of the MTM⇄HTM phase transition is marked by a dotted line. Full lines indicate Arrhenius fits of T_1. The calculated minimum of T_1 for the structure model of CsDS (MTM, Sec. III A 2) considering two-site 180° reorientations of the anions is also indicated.

In order to understand the reasons for the deviations we calculated several different MTM models to describe the reorientations of the anions. These can be separated into two different classes: (I) Small angle reorientations around the equilibrium positions of hydrogen (H_{eq}), and (II) n-site jump processes considering different populations of the sites with orientations of the anions pointing toward the faces of the coordination polyhedra [Fig. 2(a)]. The motional processes were modeled using only one common exchange rate within a model. The proton positions of a model mentioned below belong to each anion; no translational motion either of the whole anion nor of the proton was considered. To model the large amplitude of the thermal displacement parameters of H/D parallel to the c axis of the unit cell (Sec. III A 4), we chose this direction in model I to calculate the influence of small angle reorientations of the molecule on T_1. The motion was simulated by a four-site jump model (proton sites on Wyckoff position 8k). Two positions H_x enclose each of the two positions H_{eq}. All positions are placed on a circle around sulphur within the *a,c* or *b,c* plane of the unit cell. An exchange of the protons between these positions was presumed to have equal probability. A four-site jump reorientation parallel to the *a,b* plane of the unit cell was used in model (IIa). Two sets of Wyckoff position 4h describe the proton positions in this model. Model (IIb) simulates a six-site jump reorientation of the anions. In addition to the proton positions of model (IIa), Wyckoff position 4g was introduced to describe the motion of the anions.

For model (I) good agreement of calculated and measured T_1 was reached for $\angle(H_x-S-H_{eq})\approx42°$. In the case of model (II), results of calculations and measurements are in good agreement for an occupation of H_{eq} by about 60% for model (IIa) and 75% for model (IIb). The rest of proton density is equally distributed over the other positions.

The different models of motion in the MTM in CsHS, based on the NMR studies, are not immediately reconcilable

TABLE VI. Activation energies (E_a) and *attempt frequencies* (τ_0^{-1}) determined by Arrhenius fits of the proton spin-lattice relaxation times of CsHS (see Fig. 10).

	MTM	HTM[a]	HTM[b]
E_a /kJ mol^{-1}	13.5 ± 0.5	9.3 ± 0.3	13.8 ± 0.4
$1/\tau_0$ /s^{-1}	$(2.5\pm0.8)\times10^{13}$	7.1×10^{12}	⋯

[a]Reorientations of HS^-.
[b]Diffusion of cations.

with the neutron diffraction studies of CsDS (Sec. III A). However, the calorimetric investigations indicate that this is not due to an intrinsic difference between CsHS and CsDS. On the one hand, the difference could be related to the difference in sensitivity of different techniques to different aspects of dynamics.[41,42] On the other hand, there might be an influence of an amorphous phase, as mentioned in Ref. 8. This amorphous content can be removed by heating the samples to $T=473$ K for two weeks and subsequent slow cooling to room temperature.[8] Further investigations taking an improvement of the sample preparation into account will follow to determine the reasons for the observed discrepancies.

T_1 rises drastically with the MTM→HTM phase transition and increases following an Arrhenius law with temperature up to $T\approx250$ K. Probably reorientational motion of the anions dominates the spin-lattice relaxation up to this temperature. At higher temperatures a change in the mechanism of relaxation can be seen (Fig. 10). Above $T>330$ K the relaxation becomes more efficient and T_1 decreases with temperature also following an Arrhenius form. As for the temperature dependence of M_2 in the HTM, the onset of translational motion seems to be reasonable to explain the observed T_1 since the reorientations of the molecular ions are faster than at $T_{1\,\mathrm{min}}$ and a slowing of reorientations is unrealistic. A high mobility of the ions in the HTM can also be expected from the enhancement of crystal quality at high temperatures.[8] A similar behavior of T_1 was observed for MHS with $M=$ Na, K, Rb[18,20] and an increase of activation energies with an increasing radius of M favor a diffusion of the cations. Nevertheless, the activation energies are quite low for long-range translational motion in solids. A combination of low- and high-resolution quasielastic neutron scattering experiments should give information about translational motion of protons or the whole anions, respectively. High-resolution experiments are necessary to analyze the rotational part, which must be separated from the translational part.

The activation energies were determined by Arrhenius fits of T_1 for the HTM. For the MTM we used an expression following Blombergen, Purcell, and Pound[43] also, presuming a thermal activated process. The results are summarized in Table VI. The activation energy of the reorientational process in the HTM is in good agreement with results from QENS experiments.[10] The activation energies of the reorientational motion of the anions in the MTM of CsHS compared with results for the MTM of MHS with $M=$Na,K,Rb[20] show a decrease with increasing radius of the cations. This means that the softening of the coordination potential of the anions supports their reorientations, and the Cs compound follows this tendency, although the crystal structure changes from the NaCl- to the CsCl-type structure.

IV. CONCLUSIONS

Neutron diffraction, solid state ^{1}H-NMR, and calorimetric investigations were carried out in a wide temperature range on CsHS and CsDS in order to study structure and dynamics of these compounds.

Large-amplitude liberations of DS^- are indicated in a distinct anisotropy of the thermal displacement parameters of deuterium within the whole investigated temperature range. Contrary to the NaCl-typelike compounds NaDS and KDS, which have considerable anharmonicity of the coordination potential of deuterium,[17,19] a harmonic model fits well with the neutron diffraction data of CsDS. This is caused by the two-fold symmetry of the coordination potential of D in CsDS, which is more closely related to an ellipsoid describing the pdf within the harmonic approximation than the three-fold symmetry of the coordination potential of NaDS, KDS, and RbDS. Nevertheless, data from neutron diffraction show a significant influence of the coordination potential of D highlighted by the different amplitudes of librational motion in the LTM and MTM, as seen by the length of the principal axis of the thermal displacement parameters.

In the HTM an SAF model is more appropriate than a split-atom model to describe the pdf of *D*. The shape of the very smeared-out pdf still accounts for the influence of the potential of the particle involved in fast reorientational dynamics by avoiding orientations of the anions leading to high repulsive forces between Cs^+ and D^+.

An analysis of thermal displacement and lattice parameters shows precursor effects for both LTM⇄MTM and MTM⇄HTM phase transitions by a change in the temperature dependence of these parameters. The transition at high temperature is clearly of first order, as determined by calorimetric and diffraction investigations. The transition temperatures are $T=207.9\pm0.3$ K and $T=213.6\pm0.3$ K for CsHS and CsDS respectively.

The LTM⇄MTM phase transition is continuous. Order parameters, related to the displacive and the order/disorder part of this phase transition, couple bilinearly, and follow a critical law. The critical exponent is close to $n=1/4$, possibly indicating a tricritical phase transition. The transition temperature in CsDS of $T_C=123.2\pm0.5$ K determined by neutron diffraction is in good agreement with results of calorimetric investigations $T_C=121\pm2$ K. The transition of CsHS shows only a shift of the critical temperature to $T_C=129\pm2$ K and no significant change of the critical exponent was observed.

The observed second moments of the ^{1}H-NMR absorption signals of CsHS are in reasonable agreement with results of calculations based on the structure models of MTM and HTM, assuming a model of reorientational disorder of the anions provided by the crystal structure of CsDS. No NMR spectra of the LTM were measured, because of the available temperature range.

However, an analysis of spin-lattice relaxation shows a difference of measured and calculated T_1 for the crystal

structure of the MTM of CsDS, assuming two-site 180° reorientations of the anions.

Activation energies observed in *M*HS with $M=\mathrm{Na, K, Rb, Cs}$ correspond to the influence of the coordination potential by the cations on the reorientational motion of the anions. A weakening of the potential results from an increase in radius of the cations, which causes a decrease of the activation energies (cf. Refs. 17 and 20).

It seems to be reasonable that in the HTM of CsHS at $T>330$ K, spin-lattice relaxation is determined by a diffusional process as in *M*HS, with $M=\mathrm{Na, K, Rb}$. The increase of the activation energy of these compounds with increasing radius of the cations leads to the assumption of a diffusion of the cations.

V. DEPOSITED MATERIALS

The experimental heat capacities of CsHS and CsDS have been deposited with EPAPS and are available from AIP.[44]

ACKNOWLEDGMENTS

We wish to thank the German Bundesministerium für Bildung und Forschung (JA5DOR, KI5BO3), the Fonds der Chemischen Industrie, the Natural Sciences and Engineering Research Council (Canada), and the Killam Trusts for financial support of this work.

[1] H. Jacobs, U. Metzner, R. Kirchgässner, H. D. Lutz, and K. Beckenkamp, Z. Anorg. Allg. Chem. **598/599**, 175 (1991).
[2] H. Jacobs and R. Kirchgässner, Z. Anorg. Allg. Chem. **569**, 117 (1989).
[3] H. Jacobs, R. Kirchgässner, and J. Bock, Z. Anorg. Allg. Chem. **569**, 111 (1989).
[4] H. Jacobs and C. Erten, Z. Anorg. Allg. Chem. **473**, 125 (1981).
[5] L. W. Schroeder, L. A. de Graaf, and J. J. Rush, J. Chem. Phys. **55**, 5363 (1973).
[6] J. J. Rush, R. C. Livingston, and G. J. Rosasco, Solid State Commun. **13**, 159 (1973).
[7] K. Beckenkamp and H. D. Lutz, J. Solid State Chem. **109**, 241 (1994).
[8] H. D. Lutz, K. Beckenkamp, H. Jacobs, and R. Kirchgässner, J. Raman Spectrosc. **25**, 395 (1994).
[9] K. Beckenkamp, H. D. Lutz, U. Metzner, and H. Jacobs, J. Mol. Struct. **245**, 203 (1991).
[10] J. J. Rush, L. A. de Graaf, and R. C. Livingston, J. Chem. Phys. **58**, 3439 (1973).
[11] J. M. Rowe, R. C. Livingston, and J. J. Rush, J. Chem. Phys. **58**, 5469 (1973).
[12] J. M. Rowe, R. C. Livingston, and J. J. Rush, J. Chem. Phys. **59**, 6652 (1973).
[13] K. R. Jeffrey, Can. J. Phys. **52**, 2370 (1974).
[14] K. R. Jeffrey and S. L. Segel, Can. J. Phys. **54**, 1651 (1976).
[15] C. K. Coogan, G. G. Belford, and H. S. Gutowsky, J. Chem. Phys. **39**, 3061 (1963).
[16] K. R. Jeffrey and R. E. Wasylishen, Can. J. Phys. **59**, 1585 (1981).
[17] F. Haarmann, H. Jacobs, and W. Kockelmann, J. Chem. Phys. **113**, 6788 (2000).
[18] F. Haarmann, H. Jacobs, B. Asmussen, C. Nöldeke, G. J. Kearley, and J. Combet, J. Chem. Phys. **113**, 8161 (2000).
[19] F. Haarmann, H. Jacobs, M. Reehuis, and A. Loose, Acta Crystallogr., Sect. B: Struct. Sci. **56**, 988 (2000).
[20] F. Haarmann, H. Jacobs, J. Senker, and E. Roessler, J. Chem. Phys. (submitted).
[21] E. C. W. Clarke and D. N. Glew, Can. J. Chem. **48**, 764 (1970).
[22] H. Jacobs and D. Schmidt, Curr. Top. Mater. Sci. **8**, 381 (1982).
[23] W. Kockelmann, M. Weißer, H. Heinen, A. Kirfel, and W. Schäfer, Mater. Sci. Forum **332**, 321 (2000).
[24] M. Weißer, Master's thesis, Mineralogisches Institut der Universität Würzburg, 1998.
[25] A. C. Larson and B. von Dreele, University of California, Los Alamos, 1994 (unpublished).
[26] K. G. Adams, Ph.D. thesis, Universität Karlsruhe, 1999.
[27] G. Bricogne, "Fourier Transforms in crystallography: Theory, algorithms, and application," in *International Tables for Crystallography, Volume B* (Kluwer Academic, Dordrecht, 1996).
[28] W. Press and A. Hüller, Acta Crystallogr., Sect. A: Cryst. Phys., Diffr., Theor. Gen. Crystallogr. **29**, 252 (1973).
[29] W. Press, Acta Crystallogr., Sect. A: Cryst. Phys., Diffr., Theor. Gen. Crystallogr. **29**, 257 (1973).
[30] A. Hüller and W. Press, Acta Crystallogr., Sect. A: Cryst. Phys., Diffr., Theor. Gen. Crystallogr. **35**, 876 (1979).
[31] W. Press, H. Grimm, and A. Hüller, Acta Crystallogr., Sect. A: Cryst. Phys., Diffr., Theor. Gen. Crystallogr. **35**, 881 (1979).
[32] M. J. M. Van Oort and M. A. White, Rev. Sci. Instrum. **58**, 1239 (1987).
[33] K. Beckenkamp, Ph.D. thesis, Universität Gesamthochschule Siegen, 1991.
[34] J.-C. Tolédano and P. Tolédano, *The Landau Theory of Phase Transitions* (World Scientific, Singapore, 1987), Vol. 3.
[35] H. T. Stoke and D. M. Hatch, Phase Transitions **34**, 53 (1991).
[36] F. Haarmann, Ph.D. thesis, Universität Dortmund, 2001.
[37] M. J. M. Van Oort and M. A. White, J. Chem. Soc., Faraday Trans. 1 **81**, 3059 (1985).
[38] P. W. R. Bessonette and M. A. White, J. Chem. Phys. **110**, 3919 (1999).
[39] G. Bednarz, D. J. W. Geldart, and M. A. White, Phys. Rev. B **47**, 14247 (1993).
[40] R. Rosmus and W. Meyer, J. Chem. Phys. **69**, 2745 (1978).
[41] M. A. White and A. Perrott, Can. J. Chem. **66**, 729 (1988).
[42] M. A. White, R. E. Wasylishen, P. E. Eaton, Y. Xiong, K. Pramod, and N. Nodari, J. Phys. Chem. **96**, 421 (1992).
[43] N. Blombergen, E. M. Purcell, and R. V. Pound, Phys. Rev. **73**, 679 (1948).
[44] See EPAPS Document No. E-JCPSA6-117-508224 for experimental heat capacities for CsHs and CsDs. This document may be retrieved via the EPAPS homepage (http://www.aip.org/pubservs/epaps.html) or from ftp.aip.org in the directory /epaps/. See the EPAPS homepage for more information.